INFLUENCE OF ORGANIC FRICTION MODIFIERS ON SURFACE ENERGY PROPERTIES IN POLYALPHAOLEFIN (PAO) BLENDS

Article history
Received
12nd January 2025
Received in revised form
25th March 2025
Accepted
15th June 2025
Published
26th June 2025

Chiew Tin Lee[a]*, Hou Mun Ng[b], Aaron Edward Sheng Jye Teo[a], Keng Yinn Wong[b,c]

[a]Faculty of Engineering, Universiti Malaysia Sarawak (UNIMAS), Kota Samarahan 94300, Sarawak, Malaysia
[b]Faculty of Mechanical Engineering, Universiti Teknologi Malaysia, 81310 UTM Johor Bahru, Johor, Malaysia
[c]Institute for Sustainable Transport (IST), Universiti Teknologi Malaysia, 81310 UTM Johor Bahru, Johor, Malaysia

*Corresponding author
tlchiew@unimas.my

ABSTRACT

The shift towards alternative fuels like hydrogen, ethanol, and other sustainable energy sources drives the need for high-performance lubricants to handle new thermal and chemical challenges. Synthetic polyalphaolefins (PAOs) are commonly utilised due to their thermal stability, high viscosity index, and reliable low-temperature flow. This study investigates the impact of organic friction modifiers—oleic acid (OA) and stearic acid (SA)—on PAO-based lubricants' tribological and interfacial characteristics. Blends containing 0.1–0.5 wt% OA or SA were tested. Contact angle measurements indicated that the 0.3 wt% OA blend significantly improved surface wettability, achieving the lowest contact angles on glass and steel surfaces. Surface energy analysis revealed decreased surface tension and better adhesion for the 0.3 wt% OA blend. Friction testing showed that the 0.3 wt% OA blend recorded the lowest coefficient of friction; however, wear resistance largely remained unaffected. These findings indicate that OA improves frictional performance in PAO lubricants, presenting a promising avenue for optimising formulations for future energy systems.

KEYWORDS

Polyalphaolefins, Stearic Acid, Oleic Acid, Contact Angle, Friction, Wear.

INTRODUCTION

The global transition toward sustainable fuels, including hydrogen, ethanol, and biofuels, requires lubrication systems that are more efficient and durable to handle new operating environments characterised by higher moisture levels and reactive combustion byproducts. Recent developments in lubrication technology aim to enhance system integration, prolong service life, and increase environmental sustainability. This study explicitly investigates the combination of organic friction modifiers (OFMs) with polyalphaolefin (PAO) lubricants to improve their tribological performance across various industries. OFMs, such as oleic acid and stearic acid, reduce wear and friction while enhancing the formation of protective layers and boundary lubrication [1, 2]. The study conducted by Al-Quraan et al. illustrates the effectiveness of OFMs in minimising wear rates and providing surface protection under different operational conditions, validated through a four-ball tribometer [3].

The efficiency of lubricants relies on how well they wet surfaces and adhere to solids, with crucial metrics being the contact angle and surface energy [4]. These elements are essential for assessing a lubricant's compatibility with specific surfaces and significantly impact its overall performance. Digital microscopy enables continuous monitoring of wear track development, yielding valuable insights into friction and wear phenomena [5]. Specific nanoparticles serve as additives to improve lubricant performance by modifying surface characteristics and decreasing frictional coefficients, as studied by Gulzar et al. [6] and Li et al. [7]. Grasping solid substrates' total and distinct surface energies, including polar and

nonpolar components, is essential for selecting lubricants that maintain stable boundary layers and high endurance across different materials [8]. This understanding is critical when tailoring lubricant formulations for specific industrial uses, as Song and his team showed in their research on the surface energy interactions of materials like graphene [9].

While numerous studies have investigated the tribological performance of synthetic base oils and commercial additive systems, there remains a limited understanding of how naturally derived organic friction modifiers (OFMs), such as oleic acid (OA) and stearic acid (SA), affect interfacial properties like surface energy, wettability, and lubrication performance. Prior works have generally overlooked the systematic comparison of OA and SA concentrations in PAO-based blends, particularly in the context of surface energy analysis and contact angle behaviour. This knowledge gap is critical as interfacial adhesion and wetting strongly influence lubricant film formation and efficiency, especially in boundary and mixed lubrication regimes.

To address the gap, this study explores lubrication technology by examining how OFMS influences the surface energy behaviour of PAO-containing blends. By concentrating on additive synergies, the research aims to enhance the efficiency and longevity of lubricants in various industrial applications. It evaluates lubricant performance based on its ability to adhere to and spread over solid substrates, directly impacting friction. Additional contact angle measurements offer more profound insights into how lubricants interact with different substrates, illuminating specific mechanical engineering challenges that necessitate tailored lubrication systems.

Experimental Section

Materials

Durasyn 164X polyalphaolefin (PAO) was selected as the low-viscosity base oil due to its high thermal stability, low pour point (~60 °C), and good oxidative resistance. It has a kinematic viscosity of about 4 cSt at 100 °C and a high viscosity index.

Oleic acid (CAS No. 112-80-1) and stearic acid (CAS No. 57-11-4) were obtained from Sigma-Aldrich and used as organic friction modifiers. Oleic acid is a monounsaturated fatty acid that is liquid at room temperature (melting point ~13–14 °C), while stearic acid is saturated and solid at room temperature (melting point ~69–70 °C). Their structural differences influence their solubility in PAO and interaction with metal surfaces.

PAO is a lubricant base oil due to its remarkable properties, including superior oxidation resistance and thermal stability, guaranteeing dependable performance under high temperatures [10]. Coelho de Sousa Marques et al. [11] noted that PAOs can adapt to various operating conditions because of their low-temperature fluidity. Incorporating organic friction modifiers (OFMs) into PAOs enhances their tribological performance by minimising wear and friction, thus extending the life of mechanical components and improving machine efficiency [2]. The lubricant's performance is further augmented when OFMs combine with the PAO base oil to create protective tribofilms on surfaces [12]. The optimal choice for high-performance lubricants results from the advantageous effects of OFMs alongside the inherent characteristics of PAO.

Blending Process

The PAO4 base oil was blended with different concentrations of stearic acid and oleic acid at 0.1 wt%, 0.3 wt%, and 0.5 wt%. The mass of the compounds was measured using an analytical balance with a precision of 0.0001 grams. The mixing process began with an IKA RW20 digital mechanical stirrer to ensure thorough integration of the substances. The mixture was then prepared for ultrasonication, which removed dissolved gases in the lubricant, reduced cavitation, and maintained a stable film between moving surfaces. Ultrasonication also breaks down agglomerates and particles, enhancing the lubricant's effectiveness. The samples were placed in a water bath set at 70°C for two hours, then cooled before storage. There was no visible phase separation, precipitation, or turbidity over two weeks, indicating good stability under static conditions.

Viscosity and Density

The physical properties of viscosity and density were analysed. Density was assessed using the DMA4100M density meter, while viscosity was measured with the Brookfield Viscometer DV-II+Pro on blended materials at four specific temperatures. Concentrations were recorded at 15°C, 40°C, and 100°C with dynamic viscosity evaluated at 40°C and 100°C.

Contact Angle Measurement

Contact angle experiments provide essential insights into the wetting behaviour of lubricants on solid surfaces. The procedure, in accordance to the method proposed by Lee et al. [13], begins by powering on the camera and LED lights, which are connected to a laptop. The microscope lens and stage are cleaned using a non-alcohol lens wiper. The LED sensor is activated, and the HAYEAR software focuses the camera on the stage image. The sample is then positioned on the stage and aligned horizontally and vertically, maintaining a 3 mm gap between the sample surface and the syringe needle. Once the microscope is finely adjusted for a sharp image, the droplet is inspected for air bubbles, and both droplet clarity and size are confirmed. The syringe is pre-filled with the lubricant mixture, and a droplet is manually applied to the sample surface. The microscope is then refocused for 30 seconds to capture a clear image. Image analysis is conducted using the ImageJ software, and the entire measurement procedure is repeated six times for each sample to ensure accuracy and repeatability.

Surface Energy Calculation

Surface energy is crucial in determining lubricants' wetting behaviour and adhesion properties on solid surfaces. Kwok and Neumann [14] said that interpreting contact angle data offers essential information about how lubricants and surfaces interact, which is crucial for maximising tribological performance [14]. Thus, improving the efficiency and efficacy of lubricants in lowering friction and wear requires a thorough understanding of surface energy.

The Owens-Wendt model was used to calculate the surface energy components of solids and liquids, considering their dispersive and polar components. Surface energy calculation is based on two main equations.

$$\gamma_L(1+\cos\theta) = 2\sqrt{\gamma_S{}^d \cdot \gamma_L{}^d} + 2\sqrt{\gamma_S{}^p \cdot \gamma_L{}^p} \quad (1)$$

$$\gamma = \gamma^d + \gamma^p \quad (2)$$

Where
γ_L= total surface tension of the liquid
$\gamma_S{}^d$= dispersive component of the solid surface energy
$\gamma_L{}^d$= dispersive and polar components of the liquid surface energy
$\gamma_S{}^p$= polar component of the solid surface energy
$\gamma_L{}^p$= polar component of the liquid surface energy
γ= total surface tension of the liquid or the solid

It is worth noting that Equation (1) has five unknowns. To eliminate the first two unknowns related to the solid, solid surface energy (γ_S) can be calculated by measuring the contact angle of a standard liquid with known properties, diiodomethane and deionised water (Table 1). The contact angle must be measured on at least two surfaces. In this study, the surfaces were glass and steel. After obtaining the dispersive and polar component of the solid surface, solving the liquid surface tensionγ_L) also requires the measurement of contact angle on both glass and steel surfaces.

Table 1: Properties of standard liquid

Standard liquid	γ_L (mJ/m²)	$\gamma_L{}^p$ (mJ/m²)	$\gamma_L{}^d$ (mJ/m²)
Water	72.8	51.0	21.8
Diiodomethane	50.8	0	50.8

The interfacial energy (γ_{SL}) between the solid surface (steel) and the lubricant was calculated using the harmonic mean formulation derived from the Owens–Wendt model. The equation used is as follows:

$$\gamma_{SL} = \gamma_S + \gamma_L - 2\left(\sqrt{\gamma_S{}^d \cdot \gamma_L{}^d} + \sqrt{\gamma_S{}^p \cdot \gamma_L{}^p}\right) \quad (3)$$

This equation provides a quantitative measure of the adhesive interaction between the lubricant and the steel substrate. The values used for each component were derived from the contact angle measurements using standard probe liquids and the Owens–Wendt method.

Friction and Wear Testing

The described friction test methodology entails a configuration with an Arduino IDE-integrated, specially designed ball-on-disk tribometer for accurate control and data logging. First, spin-coated steel discs are fastened to the tribometer, and a cleaned steel ball is positioned for best contact. Testing circumstances are consistent thanks to the tribometer arm's alignment. The main test sequence commences with an 80g load at 500 rpm, spanning a 200-meter distance over 255 seconds while temperature variations are recorded, following a run-in test with a 60g load and 1000 rpm to check for stability. After that, tests gradually increase the weight to 160 g while maintaining the same pace. For every parameter set, exact

temperature, speed, frictional force, and time records are made.

HAYEAR and a high-resolution camera system enable the visual data collection, providing comprehensive photos of wear scars on steel balls and discs. ImageJ software makes Accurate wear track assessment possible, which offers precise quantitative analysis by translating pixel values into calibrated dimensions. Many measurements ensure reliability, and findings are compiled in Excel for further examination. The methodology employed guarantees a thorough assessment of wear and friction characteristics, which is vital for refining lubricant compositions and augmenting the longevity and performance of industrial equipment.

Results & Discussion

Density of PAO4 and Fatty Acid Blends

The density of SA and OA blended samples in PAO4 at 0.1 wt%, 0.3 wt%, and 0.5 wt% concentrations is measured. Table 2 summarises the density of these blended samples at three different temperatures: 15, 40, and 100 °C. The addition of SA and OA does not significantly alter the density of the PAO4 mixture, with variations well below 1% at all concentrations and temperatures.

Table 2: Density for PAO and fatty acid blends at different temperatures

Samples	Density (g/cm^3)		
	15 °C	40 °C	100 °C
Neat PAO4	0.8207	0.8048	0.7665
PAO4 + 0.1 wt% SA	0.8223	0.8064	0.7682
PAO4 + 0.3 wt% SA	0.8227	0.8066	0.7680
PAO4 + 0.5 wt% SA	0.8228	0.8067	0.7680
PAO4 + 0.1 wt% OA	0.8224	0.8064	0.7680
PAO4 + 0.3 wt% OA	0.8225	0.8066	0.7683
PAO4 + 0.5 wt% OA	0.8227	0.8068	0.7685

Viscosity of PAO4 and Fatty Acid Blends

Table 3 shows the viscosity of blended PAO4 samples at 40°C and 100°C. The viscosity of pure PAO4 increases with 0.1 wt% SA, slightly rises with 0.3 wt% SA, and then decreases with 0.5 wt% SA. OA increases with 0.1 wt%, slightly decreases with 0.3 wt%, and then rises again at 0.5 wt%. The viscosity index (VI) is highest with 0.3 wt% OA at 329, 2.6 times higher than neat PAO4. OA significantly influences viscosity more than SA, especially at higher temperatures. The improvement in viscosity index observed at 0.3 wt% OA may be attributed to enhanced molecular alignment and pressure-responsive flow behavior, which are also noted in biodiesel-based lubricants with polar functional groups [15].

Table 3: Dynamic viscosity for PAO and fatty acid blends at different temperatures

Samples	Viscosity (mPa.s)		VI
	40 °C	100 °C	
Neat PAO4	13.682	2.989	125
PAO4 + 0.1 wt% SA	14.515	2.919	99
PAO4 + 0.3 wt% SA	14.599	3.072	119
PAO4 + 0.5 wt% SA	14.521	2.765	66
PAO4 + 0.1 wt% OA	15.725	3.610	170
PAO4 + 0.3 wt% OA	14.761	4.687	329
PAO4 + 0.5 wt% OA	15.571	3.919	214

Contact Angle Measurement

Table 4 shows the contact angle data of neat PAO4 and the fatty acid blends on steel and glass substrates, with their corresponding droplet photo in Figure 1.

Table 4: Contact angle of PAO and fatty acid blends on steel and glass substrates

Samples	Contact Angle	
	Steel	Glass
Neat PAO4	46.78	44.78
PAO4 + 0.1 wt% SA	61.78	45.77
PAO4 + 0.3 wt% SA	53.03	45.70
PAO4 + 0.5 wt% SA	46.23	45.80
PAO4 + 0.1 wt% OA	49.02	44.77
PAO4 + 0.3 wt% OA	44.33	42.92
PAO4 + 0.5 wt% OA	47.88	47.73

The contact angle data reveal distinct trends in how stearic acid (SA) and oleic acid (OA) influence the wettability of PAO4 on steel and glass substrates. For SA, a progressive decrease in contact angle with increasing concentration suggests enhanced surface interaction and improved wettability, particularly on steel. However, the relatively unchanged contact angle on glass indicates that substrate chemistry plays a key role in modulating the effectiveness of SA.

Notably, at higher SA concentrations, crystallization occurs at room temperature, which

hinders droplet formation and precludes reliable contact angle measurement. This limitation highlights the narrow applicability window for SA incorporation and points to formulation challenges associated with phase instability.

In contrast, OA-modified PAO4 displays a non-linear response. An initial decrease in contact angle at 0.1 wt% OA indicates improved wetting. However, further increases in OA concentration lead to a rise in contact angle, suggesting saturation or aggregation effects that may hinder interfacial spreading. The optimal performance was observed at 0.3 wt% OA, with contact angles of 44.33° on steel and 42.92° on glass—values representing a significant enhancement in wettability relative to unmodified PAO4. The trend is consistent with prior reports indicating that OA can reduce interfacial tension and improve film-forming behaviour due to its polar carboxylic group [1, 12]. This behaviour implies a delicate balance between molecular orientation, interfacial adsorption, and surfactant concentration. Exceeding this optimal point likely results in micelle formation or multilayer adsorption, which could reduce the effective surface activity of OA.

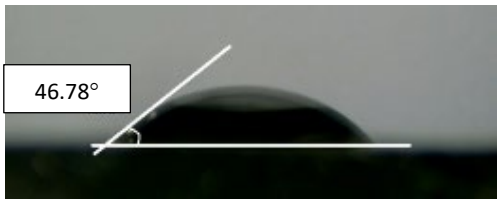

(a) PAO4 on steel substrate

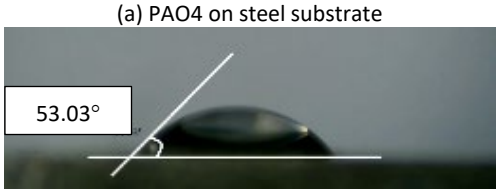

(b) PAO4 + 0.3 wt% SA on steel substrate

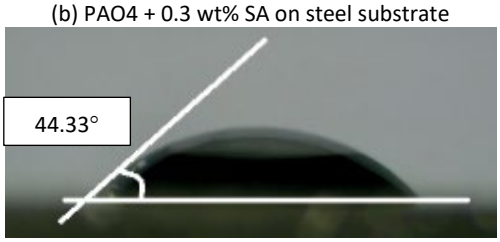

(c) PAO4 + 0.3 wt% OA on steel substrate

Figure 1: Droplet of PAO and 0.3 wt% oleic aci blends on steel substrates

Overall, these findings demonstrate that both the type and concentration of organic friction modifiers critically affect lubricant-substrate interaction. Tailoring surfactant chemistry is therefore essential for optimizing the surface affinity and tribological performance of PAO4-based lubricants, particularly in applications where interfacial adhesion governs film formation and wear protection.

Surface Energy and Interfacial Energy

The study also examines the interfacial characteristics and surface energy of PAO4 lubricants that the organic additions of OA and SA have altered. Table 5 tabulates the surface energy of the blends and the interfacial energy between them and the steel substrates.

Table 5: Surface energy and interfacial energy of PAO and fatty acid blends on steel and glass substrates

Samples	Surface Energy (mJ/m²)	Interfacial Energy (mJ/m²)
Neat PAO4	53.52	90.17
PAO4 + 0.1 wt% SA	82.88	122.07
PAO4 + 0.3 wt% SA	67.72	108.45
PAO4 + 0.5 wt% SA	50.86	86.04
PAO4 + 0.1 wt% OA	58.80	97.36
PAO4 + 0.3 wt% OA	50.72	86.99
PAO4 + 0.5 wt% OA	51.75	86.45

Table 5 highlights that neat PAO4 exhibits a surface energy of 53.52 mJ/m², reflecting moderate wettability. Adding 0.1 wt% stearic acid (SA) significantly increases the surface energy to 82.88 mJ/m², suggesting a transient improvement in surface interaction, likely due to monolayer adsorption. However, further increases in SA concentration to 0.3 wt% and 0.5 wt% result in a decline in surface energy to 67.72 mJ/m² and 50.86 mJ/m², respectively. This reduction may be attributed to molecular crowding or the onset of crystallisation, which impairs surface conformity and disrupts optimal spreading behaviour.

In contrast, oleic acid (OA) exhibits a more consistent trend. At 0.1 wt%, surface energy increases slightly to 58.80 mJ/m², but then drops to a minimum of 50.72 mJ/m² at 0.3 wt%, suggesting enhanced wetting potential. At 0.5 wt% OA, the surface energy rises marginally to 51.75 mJ/m², possibly indicating a limit in OA surface activity or partial aggregation. The lowest surface energy observed at 0.3 wt% OA aligns with its lowest measured contact angle, reinforcing its superior wetting capacity. This implies that OA, particularly at 0.3 wt%, effectively modifies the PAO4 base oil for better interfacial spreading, critical for forming stable lubricating films on metallic substrates.

The interfacial energy values further corroborate this trend. Formulations with 0.3 wt% and 0.5 wt% OA and 0.5 wt% SA exhibit lower interfacial energies compared to neat PAO4, indicating enhanced adhesive interaction with steel

surfaces. Among all, the OA3 blend (0.3 wt% OA) demonstrated the most favourable balance of low surface energy, low contact angle, and reduced interfacial energy, traits that promote efficient lubricant film formation and surface adhesion, particularly under boundary lubrication regimes.

Friction and Wear Performance

Figure 2(a) illustrates that PAO4 modified with 0.3 wt% OA (OA3) consistently exhibits lower friction forces across different normal loads at 500 rpm than neat PAO4. This decrease reflects enhanced lubrication efficiency, likely due to improved wettability and film formation at the contact interface. Additionally, Figure 2(b) confirms this trend; 0.3 wt% OA achieves a coefficient of friction (COF) of 0.057, a 57% reduction from 0.132 for neat PAO4. This significant decrease in COF highlights OA3's effectiveness in reducing shear resistance, especially within mixed lubrication regimes where interfacial chemistry is crucial. The significant reduction in friction for the 0.3 wt% OA blend is also consistent with findings by Lee et al. [16], who reported that methyl ester-based additives enhance polar interactions and boundary film strength in ester-based lubricants.

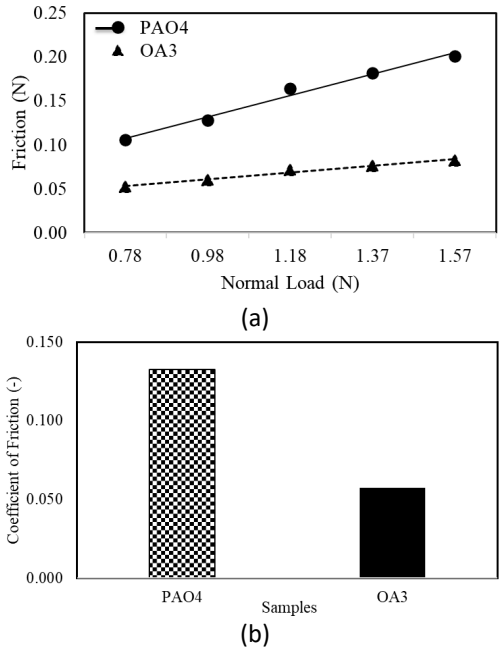

Figure 2: (a) Friction force against normal load and (b) coefficient of friction for PAO4 and 0.3 wt% OA (OA3)

The wear analysis presented in Figure 3 shows a complex trade-off. While 0.3 wt% OA decreases the wear scar diameter by about 15%, it increases the wear track width by 26%. This indicates that 0.3 wt% OA focuses more on reducing friction than providing anti-wear protection. The trend was also observed in previous studies, where OFMs primarily contributed to boundary film formation but required additional anti-wear agents for enhanced wear resistance [2,12]. The wider wear track could suggest a change in the wear mechanism, potentially transitioning from abrasive to mild adhesive wear, influenced by boundary film thickness or chemical composition variations. These results imply that although 0.3 wt% OA successfully lowers friction through surface modification, its enhancement of wear resistance is limited, highlighting the necessity for additional anti-wear additives in future formulations. It is noted that the standard deviations from three repeated tests for friction and wear were below 5% for all data points; error bars were omitted for clarity.

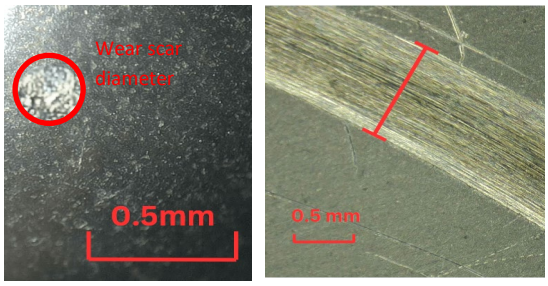

Figure 3: (a) Ball wear scar diameter and (b) disk wear track width for PAO4 and 0.3 wt% OA

Table 6: Wear properties for contact lubricated with neat PAO4 and OA3

Sample	Wear scar diameter (mm)	Wear track width (mm)
Neat PAO4	0.46	0.74
OA3	0.39	0.93

Conclusion

This study highlights the crucial influence of surface wettability on the tribological performance of PAO4-based lubricants. Among the formulations tested, 0.3 wt% oleic acid showed the best interfacial properties, achieving the lowest contact angles on steel and glass substrates. Surface energy analysis supported these results, revealing that OA3 had lower surface tension and superior spreading behaviour than neat PAO4 and stearic acid blends. Tribological tests confirmed that 0.3 wt% oleic acid significantly reduced friction forces and the coefficient of friction under various loads, demonstrating its efficiency as a friction modifier. Nevertheless, its modest improvement in wear resistance suggests that 0.3 wt% oleic acid alone might not be sufficient for overall performance;

therefore, the inclusion of additional anti-wear agents or synergistic additive systems could be required. These findings provide crucial insights for optimising PAO-based lubricant formulations, especially for advanced mechanical systems and emerging applications with sustainable and alternative fuels like hydrogen, where effective lubrication is vital under chemically and thermally challenging conditions.

Acknowledgements

This work was supported by the Ministry of Higher Education (MOHE) Malaysia's Higher Institution Centre of Excellence (HICoE) program under HICoE Research Grant R.J130000.7824.4J741.

Conflict of Interest

The author declares that there is no conflict of interest regarding the publication of this paper.

References

[1] Spikes, H. (2015). Friction modifier additives. *Tribology Letters, 60*(1), 1–26. https://doi.org/10.1007/s11249-015-0589-6

[2] Al-Quraan, R., *et al.* (2023). A methodological approach to assessing the tribological properties of lubricants using a four-ball tribometer. *Tribology International, 181*, 108118. https://doi.org/10.1016/j.triboint.2023.108118

[3] Tomala, A., *et al.* (2015). Interaction between selected MoS_2 nanoparticles and ZDDP tribofilms. *Tribology International, 90*, 454–461. https://doi.org/10.1016/j.triboint.2015.05.033

[4] Kalin, M., Polajnar, M., & Vižintin, J. (2013). The correlation between the surface energy, the contact angle, and the spreading parameter, and their relevance for the wetting behaviour of DLC with lubricating oils. *Tribology International, 66*, 225–233. https://doi.org/10.1016/j.triboint.2013.05.012

[5] Meylan, B., *et al.* (2017). A new ball-on-disk vacuum tribometer with *in situ* measurement of the wear track by digital holographic microscopy. *Surface Topography: Metrology and Properties, 5*(4), 045007. https://doi.org/10.1088/2051-672X/aa9537

[6] Gulzar, M., *et al.* (2016). Tribological performance of nanoparticles as lubricating oil additives. *Journal of Nanoparticle Research, 18*, 223. https://doi.org/10.1007/s11051-016-3524-5

[7] Li, Y., *et al.* (2019). Friction reduction and viscosity modification of cellulose nanocrystals as biolubricant additives in polyalphaolefin oil. *Carbohydrate Polymers, 203*, 1–10. https://doi.org/10.1016/j.carbpol.2018.08.053

[8] Kozbial, A., *et al.* (2014). Study on the surface energy of graphene by contact angle measurements. *Langmuir, 30*(23), 8598–8606. https://doi.org/10.1021/la501998t

[9] Song, Y., *et al.* (2019, March 14). Interaction of surface energy components between solid and liquid on wettability, and its application to textile anti-wetting finish. *Colloids and Surfaces A: Physicochemical and Engineering Aspects, 570*, 424–431. https://doi.org/10.1016/j.colsurfa.2019.03.014

[10] Dolatabadi, N., Rahmani, R., Rahnejat, H., Garner, C. P., & Brunton, C. (2020, February 7). Performance of poly alpha olefin nanolubricant. *Tribology International, 144*, 106095. https://doi.org/10.1016/j.triboint.2019.106095

[11] Coelho de Sousa Marques, M. A., *et al.* (2021). Heat capacity, density, surface tension, and contact angle for polyalphaolefins and ester lubricants. *Journal of Chemical & Engineering Data, 66*(5), 2203–2212. https://doi.org/10.1021/acs.jced.0c00871

[12] Ratoi, M., *et al.* (2013, December 3). The impact of organic friction modifiers on engine oil tribofilms. *RSC Advances, 3*(46), 24786–24794. https://doi.org/10.1039/C3RA44785E

[13] Lee, M. B., Lee, C. T., Chong, W. W. F., & Wong, K. J. (2023). Post-thermal annealed monolayer graphene healing elucidated by Raman spectroscopy. *Journal of Materials Science, 58*(25), 10288–10302.

[14] Kwok, D. Y., & Neumann, A. W. (1999). Contact angle measurement and contact angle interpretation. *Advances in Colloid and Interface Science, 81*(3), 167–249. https://doi.org/10.1016/S0001-8686(98)00087-6

[15] Redzuan, N. Q., Halid, I., & Hamdan, S. H. (2023). Analysing the lubricant rheology-pressure relation for biodiesel derived waste palm cooking oil (WPCO). *Journal of Transport System Engineering, 6*(2), 1–7.

[16] Lee, M. B., Balan, E. A., & Lee, C. T. (2023). Enhancing trimethylolpropane trioleate biolubricant with methyl laurate additive. *Journal of Transport System Engineering, 6*(2), 8–1.